Intracellular pH Changes Induced by Calcium Influx during Electrical Activity in Molluscan Neurons

ZAHUR AHMED and JOHN A. CONNOR

From the Department of Physiology and Biophysics, University of Illinois at Urbana-Champaign, Urbana, Illinois 61801

ABSTRACT Simultaneous measurements of electrical activity and light absorbance have been made on nerve cell bodies from *Archidoris monteryensis* injected with indicator dyes. pH indicators, phenol red and bromocresol purple, and arsenazo III, which under normal conditions is primarily a calcium indicator, have been employed. Voltage clamp pulses which induced calcium influx caused an absorbance decrease of the pH dyes indicating an internal acidification. The onset of the pH drop lagged the onset of Ca^{2+} influx by 200–400 ms, and pH continued to decrease for several seconds after pulse termination which shut off Ca^{2+} influx. Trains of action potentials also produced an internal pH decrease. Recovery of the pH change required periods >10 min. The magnitude of the pH change was largely unaffected by external pH in the range 6.8–8.4. The voltage dependence of the internal pH change was similar to the voltage dependence of calcium influx determined by arsenazo III, and removal of calcium from the bathing saline eliminated the pH signal. In neurons injected with EGTA (1–5 mM), the activity-induced internal Ca^{2+} changes were reduced or eliminated, but the internal pH drop was increased severalfold in magnitude. After the injection of EGTA, voltage clamp pulses produced a decrease in arsenazo III absorbance instead of the normal increase. Under these conditions the dye was responding primarily to changes in internal pH. Injection of H^+ caused a rise in internal free calcium. The pH buffering capacity of the neurons was measured using three different techniques: H^+ injection, depressing intrinsic pH changes with a pH buffer, and a method employing the EGTA-calcium reaction. The first two methods gave similar measurements: 4–9 meq/unit pH per liter for pleural ganglion cells and 13–26 meq/unit pH per liter for pedal ganglion cells. The EGTA method gave significantly higher values (20–60 meq/unit pH per liter) and showed no difference between pleural and pedal neurons.

INTRODUCTION

Direct and precise measurements of neuron intracellular pH *in situ* were first reported by Caldwell (1958) for squid axon. His values of resting pH, ~7.0, although somewhat lower than subsequent measurements, demonstrated that

J. GEN. PHYSIOL. © The Rockefeller University Press · 0022-1295/80/04/0403/24 $1.00 403
Volume 75 April 1980 403–426

internal $[H^+]$ is a regulated quantity and that H^+ is not at equilibrium across the plasma membrane under normal resting conditions. More recent studies on squid axon (c.f. Spyropoulos, 1960; Boron and DeWeer, 1976) have placed resting pH at ~7.3, whereas the studies of Thomas (1974, 1976) on snail neuron somata have given a value of 7.45. Although internal pH is rather insensitive to changes in external pH, changes of 0.3–0.6 U can be induced by exposure to CO_2, NH_4^+, or by injection of bicarbonate or hydrogen ions (c.f. Caldwell, 1958; Thomas, 1974; Boron and DeWeer, 1976).

A certain amount of recent interest has focused on pH changes which occur in conjunction with physiological function, for example, the acidification that occurs in photoreceptors following exposure to light (Brown et al., 1976, 1977; Brown and Thomas, 1978). Meech and Thomas (1977) have recently demonstrated a pH decrease in *Helix* neurons following the injection of Ca^{2+}, an ion species whose influx increases during excitation in these neurons. In a previous report (Ahmed and Connor, 1979 *a*), characteristics of calcium movement analyzed by means of the metallochrome dye, arsenazo III, were described. Prominent in some of the absorbance records, especially those of post-influx periods, were indications that the dye was possibly responding to internal pH changes as well as changes in calcium concentration. The present study was undertaken to determine whether pH was changing measurably as a result of voltage clamp tests or action potentials and, if so, whether the change could be related to changes in internal calcium concentration. Most of the pH measurements reported here have been made colorimetrically using the indicator dyes phenol red and bromocresol purple in order to gain time resolution over the possibly more accurate pH microelectrodes which have fairly slow response characteristics. Preliminary reports of this work have been made (Connor and Ahmed, 1978, 1979; Ahmed and Connor, 1979 *b*).

MATERIALS AND METHODS

Central neurons from specimens of *Archidoris monteryensis* and *Archidoris odhneri* collected from the waters around Friday Harbor, Wash., were used in these experiments. All data reported, except that of Fig. 1B, were obtained from *A. monteryensis*. Animals were maintained in artificial seawater at 12°C for periods up to 3 wk prior to use. Dissection procedures and a diagram of reidentifiable neurons have been given in a prior communication (Connor, 1979). Physiological saline compositions are given in Table I. The voltage clamp experiments illustrated in this article were carried out in TEA saline to reduce outward membrane current (see Connor, 1979) and improve voltage control. Also, optical transmittance changes were sometimes noted after large outward currents had been evoked. These changes were nearly wavelength independent (500 nm $< \lambda <$ 700 nm) and in the opposite direction to the pH dye responses. TEA saline and the avoidance of membrane potentials $>+$ 80 mV eliminated this signal in most cases. Action potential records were made in normal saline. Trypsin was used in most experiments to facilitate the removal of the ganglion sheath but every type of experiment was carried out at least once without the enzyme to verify that there were no significant artifacts arising from the treatment. All experiments were run at 12°C.

The experimental apparatus for single wavelength measurements has been described previously (Ahmed and Connor, 1979 *a*) except for the following modifications.

A 55 W tungsten-halogen lamp (H-3, Philips Electronic Instruments, Mahwah, N. J.), run from a regulated 12 V supply, was used to generate the light beam for absorbance measurements. A second photomultiplier tube (type R761, Hamamatsu Corp., Middlesex, N. J.) was added to the system to monitor the incident light beam at a spot adjacent to the experimental neuron. Both the incident and transneuron light signals were piped to the respective photomultipliers through 2 in. lengths of 10-mil plastic light guides (Crofon-Dupont Chemical Co.). Photomultiplier outputs were low-pass filtered with a time constant of 50 ms unless noted. Dual wavelength measurements (Fig. 11) were made using interference filters (Corion Corp., Holliston, Mass.) mounted on a rotating wheel (see Chance, 1972; Brinley and Scarpa, 1975). Rotation speed was 1 rps. For the dual wavelength measurements a time constant of 1.5 s was used.

The following indicator dyes, all obtained from Eastman Chemicals (Rochester, N. Y.), were tested as indicators of cytoplasmic pH: bromothymol blue, bromocresol

TABLE I
EXPERIMENTAL SOLUTIONS

Ions	Normal saline	TEA saline	Ca-free saline	Ba saline	NH_4 saline	Internal saline
			mM			
NaCl	490	390	390	390	480	50
KCl	8	8	8	8	8	350
$MgCl_2$	20	20	35	50	20	3
$MgSO_4$	30	30	30	0	30	0
$CaCl_2$	15	15	0	0	15	0
$BaCl_2$	0	0	0	15	0	0
MOPS (H-Buffer)	10	10	10	10	10	20*
TEA-Cl	0	100	100	100	0	0
NH_4Cl	0	0	0	0	10	0
pH	7.4	7.4	7.4	7.4	8.0	7.2

* In internal solutions morpholinopropane sulfonic acid (MOPS) was excluded in instances where pH changes were being measured.

purple, brilliant yellow, neutral red, cresol red, and phenol red. Of these, phenol red (PhR) and bromocresol purple (BCP) were the most satisfactory in terms of absorbance signal magnitude and the uniformity of intracellular distribution as evidenced by visual inspection. Some of the other dyes, most notably bromothymol blue, tended to form a structured pattern of color near the injection site giving the visual impression that the dye was clinging to intracellular organelles.

BCP and PhR (sodium salts) were freed of metal contaminants by four exposures to fresh Chelex 100 resin (Bio-Rad Laboratories, Richmond, Calif.). Some differences in dye lots were encountered. Dye solution was separated from the resin by centrifugation between each exposure. Both dyes had toxic effects when used directly as supplied. Cells survived well for 6–8 h when injected with the purified dyes. Dyes were injected into the cells either by pressure injection of solution at pH 7.2 or by interbarrel iontophoresis. Iontophoretic current was applied as 0.9-s pulses, 200–400 nA amplitude repeated at 1 Hz. The return electrode was filled with 3 M KCl. Internal phenol red concentration was calibrated by mixing $Na_2{}^{35}SO_4$ (New England Nuclear, Boston, Mass.) with dye solution (100 μCi/18.2 μmol dye) and injecting the mixture under pressure (see Coles and Brown, 1976). Neuron absorbance was moni-

tored during injection at 560 nm, and after the experiment the cell was trypsin-digested, and the ^{35}S content was determined using a liquid scintillation counter (ISOCAP 300, Nuclear Chicago). Cell volume and light pathlength determinations were routinely made by inspection at × 80 magnification. The isotope injection technique was also used to determine injected EGTA and MOPS concentrations. As a check against gross inaccuracies in the cell diameter measurement, three neurons were injected with ^{35}S, quick-frozen, and then sectioned at 20 μm and dried at temperatures below −30°C. Autoradiographs were then made of the sections and cell volume determined from the film image.

Molar extinction coefficient (ϵ) and extinction coefficient changes ($\Delta\epsilon$) as a function of pH change (ΔpH) were determined in a Cary 118c spectrophotometer for phenol red at 0.25, 0.5, 0.75, and 1 mM concentrations (1-mm pathlength) in the internal saline mix (Table I). The reference solution was at pH 7.2. At pH 7.2 the mean value of ϵ for all dye concentrations was 1.48×10^4 ($\pm 0.06 \times 10^4$ SD) $M^{-1} \cdot cm^{-1}$, and for small pH changes around 7.2 (±0.2) the mean indicator constant $C_I = \Delta pH/\Delta\epsilon$ was 4.7×10^{-5} M·cm·unit pH (dye lot D6A). No systematic changes in these values were noted with dye concentration changes. Increasing Ca in the internal saline mix from nominally Ca-free to 5 mM had no measureable effect on the absorbance of either pH dye. All in vitro pH measurements and standardizations were made using a Corning Digital III pH meter (Corning Glass Works, Corning, N. Y.) with a Thomas 4094-L15 electrode. The meter settings were checked before and after each series of measurements using commercial standards (0.1 M concentration) at pH 4.0, 7.0, and 9.0 (Curtin Matheson Scientific, Houston, Tex. or Beckman Instruments, Inc., Fullerton, Calif.).

The H^+:Ca^{2+} stoichiometry of the partial reaction,

$$EGTA + Ca^{2+} \rightleftharpoons Ca\ EGTA + nH^+,$$

was determined titrimetrically using a Radiometer (Copenhagen, Denmark) type TTT1C automatic titrator. EGTA concentrations of 0.88, 2.5, 12, and 18 mM mixed with internal saline solution (Table I) were tested over a range of added $CaCl_2$, 25–300 μM. Under these conditions the ratio of H^+ released to Ca^{2+} added was 2:1 (best fit slope of data 2.07) with no significant variation with EGTA concentration. Fig. 1 A is a plot of intracellular phenol red concentration estimated by two methods for 10 cells; the ordinate is the phenol red concentration estimated from the extinction coefficient at 560 nm, assuming pH_i of 7.2 (see Results), and the abscissa is the concentration estimated from the isotope mixture method. Absorbance was measured at a pH-dependent wavelength ($\lambda = 560$) instead of 460 nm, the isosbestic wavelength (see Fig. 1 B), by necessity because the neurons absorb heavily in the blue wavelengths (see Fig. 1, Ahmed and Connor, 1979 *a*). Optical measurements are expressed as absorbance changes:

$$\Delta A = \log \frac{I_x}{I_x - I_A},$$

where I_x is the photomultiplier signal before the test and I_A is the change in this signal. An equivalent pH change has been computed for some neurons using the relation

$$\Delta pH = C_I \cdot \Delta\epsilon = \frac{C_i \Delta A}{l \cdot [I]},$$

$\Delta\epsilon$ being the extinction coefficient change of the dye; C_I, the indicator constant

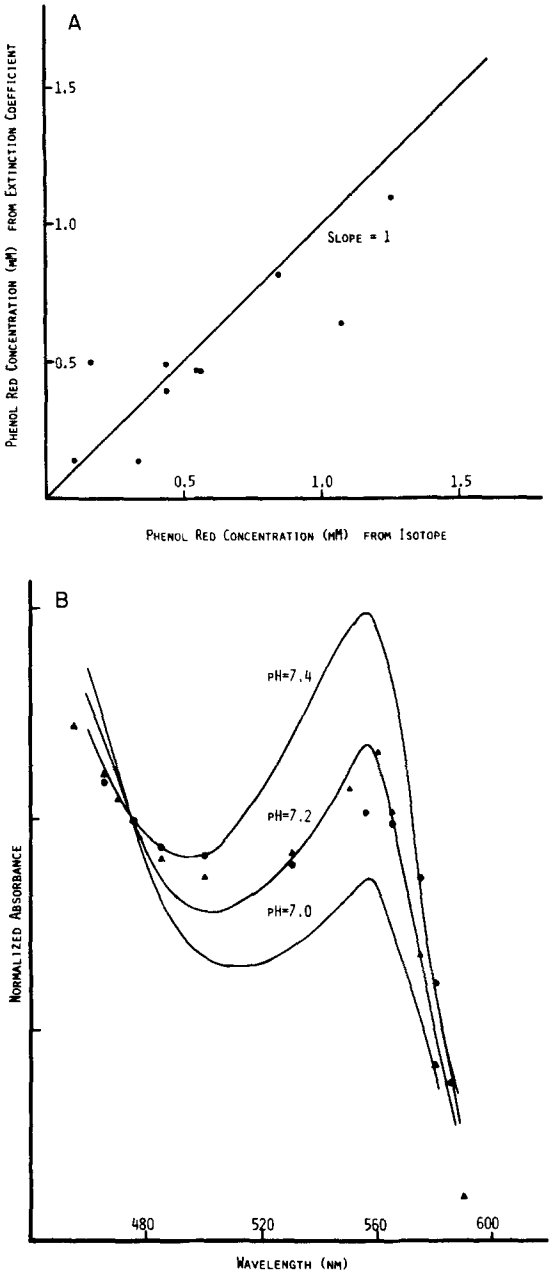

FIGURE 1. (A) Comparison of intracellular phenol red (PhR) concentrations. Ordinate: dye concentration estimated from extinction coefficient measurement at 560 nm assuming an internal pH of 7.2. Abscissa: dye concentration in same neurons estimated from ^{35}S content. (B) Data points: *in situ* spectra of PhR in two neurons. Continuous curves: in vitro PhR spectra measured in artificial internal saline.

($\Delta pH/\Delta\epsilon$); [I] the dye concentration; l the light pathlength, taken here to be the cell diameter. Equivalent pH data were not obtained for all experiments because of the necessity of leaving the optic fiber in the same position before and after dye injection and this was not always possible. Most of the absorbance changes reported here are quite small, 10^{-4} to 10^{-3} ΔA, and differences in the signal-to-noise ratio are apparent in the various records, due largely to differences in building vibration levels.

pH microelectrodes were purchased from Microelectrodes, Inc. (Londonderry, N. H.) in order to have an independent check on dye behavior *in situ* and to determine whether injecting the dyes had large or irreversible effects on pH_i. The sensing tip of the electrode was ~35 μm in length, making it suitable for use with only the larger neurons, those having diameters >400 μm. Most recordings were attempted from the giant neuron in the right pleural ganglion (RPl_G) which generally had a diameter in excess of 500 μm. Penetration of the cell by the pH electrode was carried out in a Ca-free saline at pH 8.4 to minimize Ca^{2+} and H^+ entry. The following criteria were used to establish full insertion of the sensing tip: (*a*) a brief pH change in the external bath of 1 U (from 8.4 to 7.4 or from 7.4 to 6.4) produced at most a 0.1 U change in the electrode measurement. (*b*) The pH electrode sensed at least 95% of an imposed change in transmembrane voltage. (*c*) After a brief change of the normal saline at pH 7.4 to a saline at pH 8.0 containing 10 mM NH_4Cl (see Table I) the electrode indicated an alkalinization of 0.2 to 0.4 U (see Thomas, 1974; Boron and DeWeer, 1976). One such NH_4Cl experiment is illustrated in Fig. 2 B. The pH electrode was standardized after each use by measuring its output in saline (300 mM KCl, 100 mM NaCl, 2 mM $MgCl_2$, 10 mM morpholinopropane sulfonic acid [MOPS]) at pH 6.4, 7.4, and 8.4. The electrodes had a sensitivity of 52 mV/unit pH over this range at 12°C.

The pH electrode preamplifier was constructed from a varactor-bridge operational amplifier (model 311, Analog Devices Inc., Norwood, Mass.) having an input impedance of 10^{14} Ω and a gain of 10. Transmembrane voltage (×10) was subtracted from the pH electrode signal using an instrumentation amplifier (Analog Devices, model AD522). The output of the AD522 was generally read from a 3½ digit panel meter (Analog Devices, model 2021) but was sometimes displayed on one channel of a two-channel penwriter (Brush model 240, Gould, Inc., Instruments Div., Cleveland, Ohio).

RESULTS

Resting pH and Indicator Dye Controls

Although the measurement of resting pH was not a major aim of these experiments, it was necessary to determine an approximate intracellular value for the neurons used under normal experimental conditions. A number of attempts were made to determine resting pH colorimetrically in the neurons of *Archidoris monteryensis*, but this technique was not successful because the native absorbance of the neurons is extremely large at wavelengths between 450 and 500 nm (Ahmed and Connor, 1979 *a*) where the isosbestic points of phenol red (470–480 nm) and BCP (480–490 nm) lie. Several specimens of the white dorid, *Archidoris odhneri*, were obtained and intracellular dye spectra were run on the relatively pigment-free neurons of these animals as a check for gross irregularities in the *in situ* dye spectrum. In Fig. 1 B phenol red spectra for two neurons (data points) are shown superimposed upon in vitro phenol red spectra (continuous curves) run with the same apparatus. There is

fair agreement between the spectra but the *in situ* absorbance is unaccountably large in the band from 490 to ~530 nm. The ratio A_{560}/A_{475} is consistent with an internal pH of ~7.2. Measurements using pH microelectrodes were at-

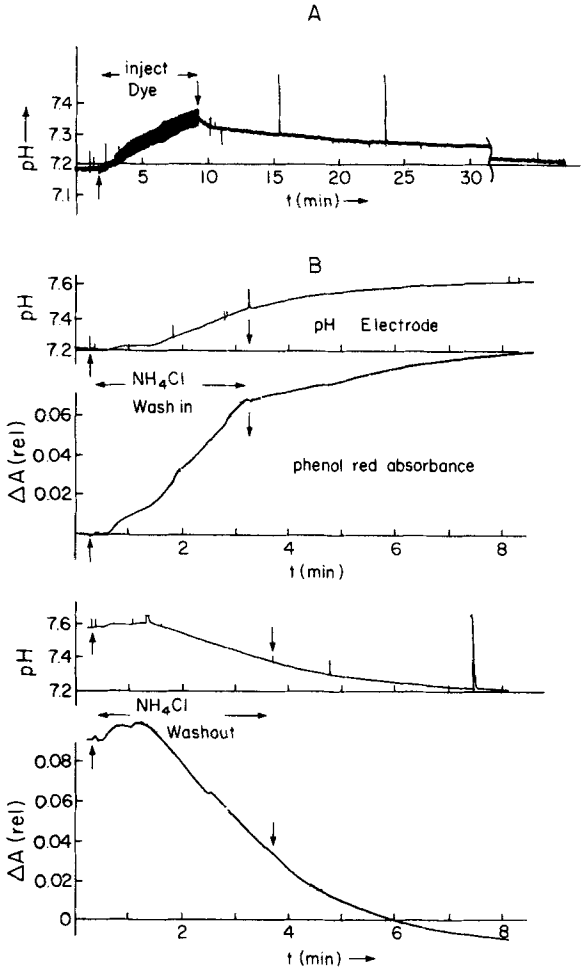

FIGURE 2. (A) pH change monitored by microelectrode during the injection of phenol red. Arrows mark onset and end of iontophoretic pulse train. 20 min of recording removed at the break at right hand side of trace. (B) Dual tracking of a pH change induced by NH_4Cl (upper records) and its recovery (lower records). Upward deflection indicates pH increase in both traces. Arrows mark onset and termination of solution flow. Noise in the optical trace during solution changes is due to slight fluid level fluctuations.

tempted on 15 neurons from *A. monteryensis*. Of these, three were acceptable in terms of the physiological conditions of the cell following penetration: i.e., $V_{rest} < -40$ mV, spike overshoot of +30 mV or greater, and cell either quiescent or firing spontaneously at a rate less than 1/s. Internal pH values

for these neurons, all RPl_G, were 7.2, 7.18, and 7.23 after a 4-mV correction for tip potential change of the reference electrode upon going from the extracellular saline to the cytoplasm (see Cole and Moore, 1960). These values are lower than those given by recent studies on other giant neurons, e.g., a mean pH of 7.45 in *Helix* neurons (Thomas, 1974), and in squid axon a mean value of 7.28 (Boron and DeWeer, 1976) and 7.35 (Spyropoulos, 1960). Although species differences and measurement errors in the present experiments are not ruled out, the above differences are not unexpected given that our studies and all the studies cited were run at different extracellular pH (pH_e). Spyropoulos (1960) and Thomas (1974), who reported the highest pH_i values, made measurements in saline at pH 8; Boron and DeWeer (1976) used pH 7.6–7.8, whereas our standard value was 7.4. Although pH_i of nerve and muscle cells is remarkably insensitive to pH_e for short time periods (c.f. Spyropoulos, 1960), when exposure periods are longer than 20 min there has been a direct and appreciable dependence shown in a number of cases. For example, the data of Paillard (1972) for *Carcinus* muscle show a $\Delta pH_i/\Delta pH_e$ of 0.3–0.4 for $5 \leq pH_e \leq 8$, while data from rat diaphragm taken by the DMO method showed a value of around 0.6 (Waddell and Bates, 1969). Thomas (1974) has shown an ~0.12 U decrease in pH_i of *Helix* neurons 10 min after changing the external saline from $pH_e = 8$ to $pH_e = 7$. The ΔpH_i had not reached steady state for the exposure time used, however. Other factors which could contribute to differences between reported pH_i values, such as temperature and CO_2 levels, have not been investigated at this time.

Iontophoretic injection of indicator caused a small, reversible change in pH as illustrated in Fig. 2 A for phenol red. In the experiment shown the neuron had been impaled with three microelectrodes (pH, voltage, and current) and allowed to equilibrate for 30 min. A fourth microelectrode containing phenol red was then inserted and the injection begun. For this experiment the dye amount injected was approximately twice the normal dose and the neuron had a pronounced red-orange color at the end of the injection period. The internal pH increase resulting from the dye injection was 0.18 U, the largest change observed in this type of test. Injection of dye to the normal concentration range (0.5–1 mM) produced a perturbation of less than 0.1 U. In all cases the pH increase was transient with recovery times of around 30 min. A transient hyperpolarization of 5–10 mV accompanied iontophoretic injection of either PhR or BCP, but not pressure injection. Both hyperpolarization and pH change decayed with about the same recovery time. Although the point was not tested, iontophoretic injection of the dyes should have caused a greater change in pH_i than pressure injection because in the former case the dye is injected as an anion and will bind H^+ from the cytoplasm whereas in the latter case the injected solution has been titrated to near the resting pH_i.

Records from a cell exposed to 10 mM NH_4Cl are given in Fig. 2 B to show that the indicator dyes respond to changes in pH_i and to give a comparison of the pH change produced by dye injection with changes produced by other means. The pH changes were tracked by both absorbance and electrode techniques. As previously demonstrated (c.f. Thomas, 1974; Boron and

DeWeer, 1976), NH_4Cl induces a large intracellular alkalinization, and, upon washout, pH drops to a value below the initial level. For the conditions employed here (10 mM NH_4Cl at pH 8) the internal pH as determined by microelectrode increased by 0.37 U. The phenol red absorbance showed the same sequence of pH changes and the pH increase estimated from the dye absorbance change was 0.24 U. Both tracking methods showed an undershoot of the initial pH after the return to normal saline, although the record of Fig. 2 B is not long enough to show this clearly for the electrode trace. It should be noted that it was more difficult to make dye concentration measurements accurately with the additional pH electrode apparatus present.

pH Changes Associated with Electrical Activity

Fig. 3 A illustrates the characteristics of BCP and PhR absorbance changes under voltage clamp. The behavior of both dyes was very similar. In each example an absorbance decrease (shown as a downward deflection) developed 200–300 ms after the onset of the voltage clamp pulse and continued well after the pulse termination (see Fig. 5 A). The delayed onset and continuing absorbance change were uniformly observed in all the neurons tested. Absorbance changes were also recorded during and after a train of action potentials (see Figs. 5 and 9). Spectra of the absorbance change for each pH dye are given in Fig. 3 B. To obtain the data points, a 1.3-s pulse to +20 mV was repeated at 3-min intervals, and the absorbance change was measured at the wavelengths shown. In each case the spectra are in close agreement with pH difference spectra for the appropriate dye in vitro which are plotted as solid curves in the figure. Owing to the large native absorbance of the cells below 500 nm, measurements near the isosbestic points of each dye are less reliable than those at higher wavelengths. Recordings similar to those of Fig. 3 A were obtained from a total of 60 neurons, a population which included at least two samples from each of the different identifiable giant neurons. Spectra were taken on eight neurons.

In the three experiments where successful penetrations were made, the pH microelectrodes also indicated an acidification after electrical activity. In these experiments V_m was clamped to −40 mV and a stable pH-V_m difference voltage established (±0.1 mV). V_m was then pulsed to +20 mV for 1.3 s or a train of 20–30 action potentials was fired under constant current stimulation, whereupon V_m was reclamped to −40 mV. The digital meter output was read 20–25 s after termination of activity to allow the pH electrode output to come to equilibrium and showed a change of 0.3–0.5 mV corresponding to an acidification of 0.004–0.008 pH U (allowing for 0.1 mV base-line error). There was no time-course information about the onset of the pH change because of the long electrical time constant of the pH electrode.

As a second verification that the indicator dyes are measuring cytoplasmic pH change and, additionally, that the observed time-course was not badly distorted, EGTA was injected into 15 neurons preloaded with either BCP or PhR. No pH buffer was added to the EGTA solution. Upon binding with Ca^{2+}, the EGTA should release H^+, according to the partial reaction EGTA

+ $Ca^{2+} \rightleftharpoons$ Ca·EGTA + nH^+. Therefore, during a voltage clamp pulse, calcium influx should cause a nearly immediate and continuous pH decrease, reflecting the maintained calcium influx (see Ahmed and Connor, 1979 *a*). Fig. 4 A shows a BCP absorbance change with simultaneously recorded membrane current before and after EGTA injection to a concentration of ~1 mM. The responses shown are for identical voltage pulses. The absorbance change became roughly five times larger after injection. In this situation, as opposed to the control run, the absorbance decrease began within a few

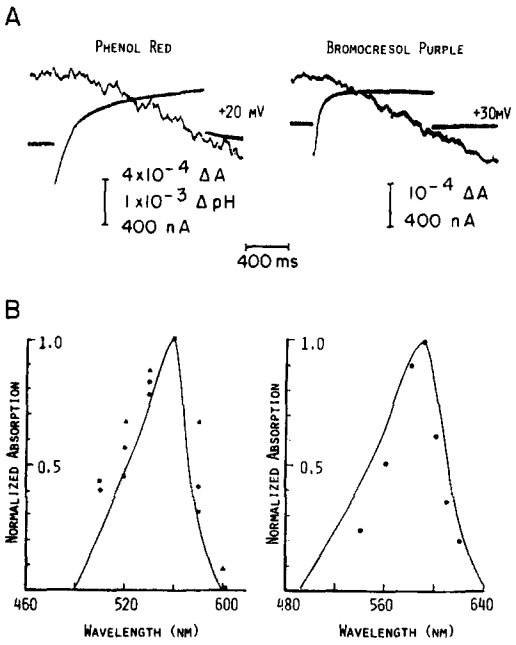

FIGURE 3. (A) Dye absorbance changes (upper traces) during voltage clamp pulse recorded from a neuron loaded with PhR (left column) and a second neuron loaded with BCP (right column). Downward deflection indicates an absorbance decrease and pH decrease. Simultaneous membrane current is shown in the lower traces. Neurons bathed in TEA saline. (B) Normalized action spectra for PhR and BCP loaded neurons (data points), three experiments for PhR, one for BCP. Continuous curves are the in vitro difference spectrum for each dye for a pH change from 7.4 to 7.2. Cells: PhR, RPe_1; BCP, $LP\prime_1$.

milliseconds of the pulse onset, and slowed soon after the pulse termination; i.e., it mirrored the time-course of Ca entry. The absorbance change during the pulse was nearly a straight line indicating a steady evolution of H^+. The spectral dependence was the same as that of the control absorbance change, i.e., consistent with a pH drop. The membrane current was inward-flowing for the duration of the pulse, indicating that the EGTA had bound most of the entering calcium thereby preventing activation of Ca-dependent potassium conductance. Previous work on these neurons (Ahmed and Connor, 1979 *a*; Connor, 1979) has shown that in the presence of 100 mM TEA, the

only appreciable outward current during voltage clamp pulses is the calcium-activated potassium current (Meech, 1974), and that effective buffering of internal calcium prevents activation of this current. Under these conditions voltage clamp current remains inward as in the records of Fig. 4.

Both the control absorbance changes and those occurring with EGTA were reduced by the injection of pH buffers, down to a level below the system resolution if the quantity of buffer was sufficient. The amount of buffer necessary to eliminate detectable pH changes in EGTA-injected cells was surprisingly high in view of the levels many investigators have used to "pH-

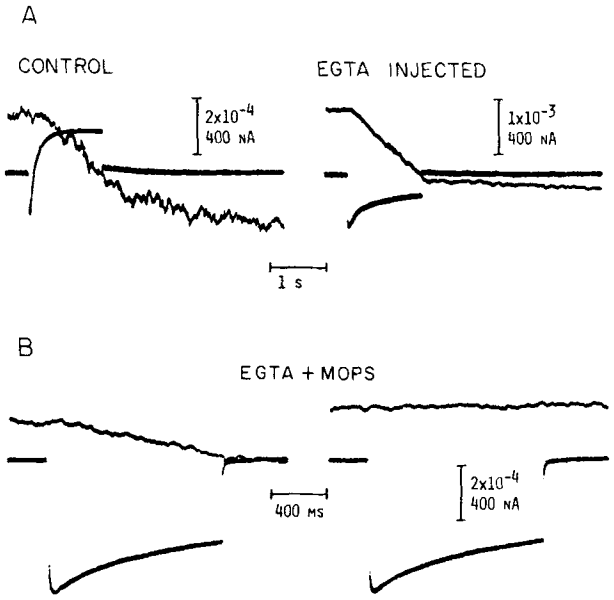

FIGURE 4. (A) BCP absorbance (upper traces) and membrane current (lower traces) during voltage pulses to +20 mV before and after EGTA injection. (B) BCP records from a second neuron injected with MOPS-EGTA mixture at an 8:1 ratio (left panel). Records of right panel were taken from the same neuron following a subsequent injection of pure MOPS. All data taken in TEA saline. Cells: LPe_2 in A; LPl_2 in B.

clamp" neurons. A commonly reported molar ratio of EGTA:buffer is 1:1 (c.f. Meech, 1974), which we found to be ineffective, at least where MOPS or imidazol were concerned. Fig. 4 B is illustrative of experiments in which EGTA:MOPS mixtures at pH 7.2 were pressure-injected at various molar ratios. As shown in the left panel of Fig. 4 B even a ratio of 1:8 left a sizeable absorbance change. Following the run shown in the left panel, pH buffer alone was pressure injected from an electrode filled with 1 M MOPS at pH 7.2. With this subsequent injection it was possible to eliminate the dye absorbance change (see Fig. 4 B right panel). There was no calibration made of the total quantity of MOPS injected in this series. However, internal MOPS concentrations that caused partial suppression of pH changes are given in

Table II. It should be noted that there was no change in the membrane current record upon the achievement of pH clamp.

Absorbance Base Line and pH Recovery

Both the BCP and PhR absorbance underwent a slow decrease during the course of experiments. In a 60-s period this base-line absorbance shift was generally $<10^{-3}$ ΔA, and in some cases was negligible. A portion of the drift is probably due to loss of dye into the external medium since both dyes are apparently soluble in the membrane phase. In fact, diffusion loading of cells by BCP has been used in some studies (c.f. MacDonald and Jöbsis, 1976). It is also possible that part of the slow absorbance decrease is due to a true pH decrease as in Fig. 2 A where the recovery from dye injection required quite a long time.

The base-line absorbance change and the recovery phase of the signal following voltage stimulation are illustrated in Fig. 5 for two neurons given both voltage clamp and action potential stimuli. The base-line absorbance change (dashed line) was determined by extrapolation of the absorbance signal from a 4-min period preceding stimulation. Cells were bathed in normal saline for these records as TEA appeared to slow the recovery phase somewhat. The first panel of Fig. 5 A illustrates a response to two identical voltage clamp pulses (+30 mV, 2 s) applied 3 s apart. Approximately two-thirds of the absorbance change, over the base-line change, occurred after the pulse termination. The spread between extrapolated base line and the absorbance signal continued to increase for ~1 min, about the same period as required for an arsenazo III signal to reach a recovery plateau following an influx of calcium (see Fig. 10, Ahmed and Connor, 1979 *a*). Where the stimulus was mild, as illustrated by the voltage clamp pulses in Fig. 5 A, the recovery phase caused only a retardation of the steady base-line drift. A more demanding stimulation of the same cell, such as the long spike train in Fig. 5 A (2.5 spikes/s for 2 min) produced a much larger pH change and a recovery phase which gave an absolute absorbance increase for a transient period. Approximately 30 min after the spike train termination, the absorbance signal had resumed its downward drift. Fig. 5 B illustrates a spike train response (3 spikes/s for 150 s) for a second cell which had a steeper initial base-line drift. Clearly the pH recovery is a slow process requiring periods >10 min.

The records of Fig. 5 illustrate the difficulty in maintaining a long-term stable base line, even a steadily changing one, in a normal experimental situation. Generally the total experimental time on a neuron was kept to under 3 h in order to minimize deterioration, but it was desirable to run more than three or four tests on a given cell. Consequently, stimuli were usually applied before complete recovery had occurred. This factor accounts for the relatively small initial slope for the spike train record of Fig. 5 A which was begun only 8 min after a preceding, shorter train. The voltage clamp run of Fig. 5 A was taken only 15 min after dye injection and shows a greater than normal base-line drift.

pH Change Is Dependent upon Ca^{2+} Influx

The pH change during voltage clamp pulses detected by either BCP or PhR vanished when calcium was removed from the external medium. Fig. 6 A

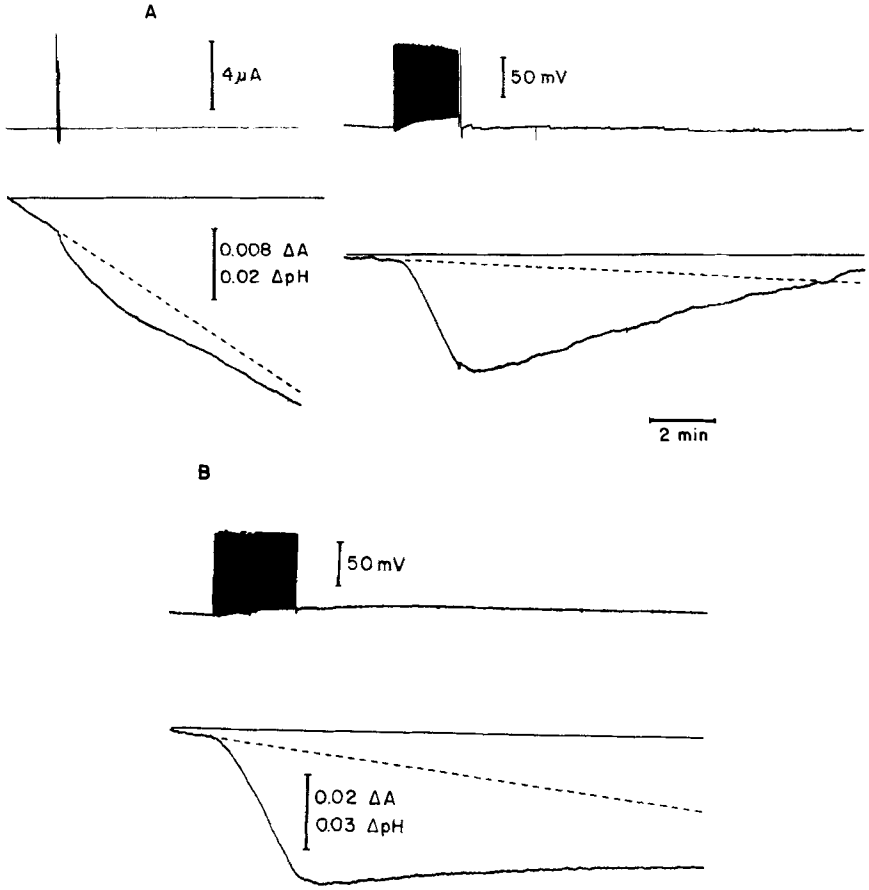

FIGURE 5. (A) Extended time-course records of PhR absorbance with voltage clamp stimulus (left panel) and spike train activity (right panel). Current and voltage are displayed in upper traces. Two sequential voltage pulses were applied (+30 mV, 2-s duration with a 3-s interval). The spike train duration was 2.5 spikes/s for 2 min. Horizontal orientation is given by solid lines on the absorbance traces while dashed lines are extrapolations of absorbance base line in the 4-min period preceding electrical activity. (B) Absorbance change associated with a spike train in a second neuron. Absorbance records low pass filtered, τ = 300 ms. Cells: LPl_2 in A; RPl_G in B.

illustrates this effect and the recovery upon calcium restoration. The absorbance signal immediately before the pulse onset is shown in the top trace of each panel. Upon exposure to the zero calcium saline with the cell clamped to its resting potential, dye absorbance increased slightly (alkalinization) for

several minutes while restoration of normal saline resulted in a slow downward drift in absorbance. Complete abolition of the pulse-induced pH change as shown in the figure developed only after several pulses had been applied. This effect was noted even after the cell was allowed equilibration for several minutes in the Ca-free EGTA saline. We are not able to say at this time whether this indicates a tightly membrane-bound fraction of calcium, or calcium remaining in the interstitial spaces near the base of the soma where small neurons and their processes are sometimes clustered, making a potentially slow diffusion compartment.

The magnitude of the pH change during and after a voltage clamp pulse

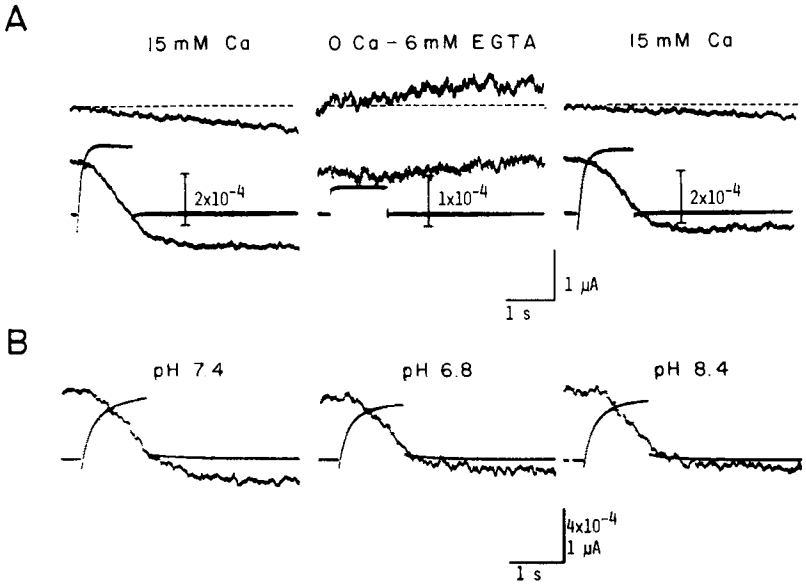

FIGURE 6. (A) Effects of external calcium depletion on pH response (PhR indicator) and membrane current. Upper absorbance records show rate of baseline drift immediately before each pulse. (B) PhR absorbance change and membrane current during identical voltage pulses (+20 mV) at three values of external pH. All records made in TEA saline. Cells: LPe_1 in A; RPe_1 in B.

was not markedly dependent on external pH. Fig. 6 B shows the pH change and membrane current associated with three identical voltage pulses in media at pH 7.4, 6.8, and 8.4. The records were taken after a 15-min equilibration at the ambient pH. Internal pH is somewhat dependent on external pH (c.f., Thomas, 1974) making the equilibration period necessary to allow the baseline pH to stabilize partially.

Fig. 7 A shows a plot of pH indicator absorbance change vs. V_m during voltage clamp pulses assembled from data of five cells. Absorbance changes were measured for pulses 1.3 s in duration, and data were normalized to facilitate comparison. A plot of arsenazo III (arIII) absorbance changes (normalized) for five other cells is given in Fig. 7 B. These absorbance increases represent calcium influx during voltage clamp pulses. The similarity between

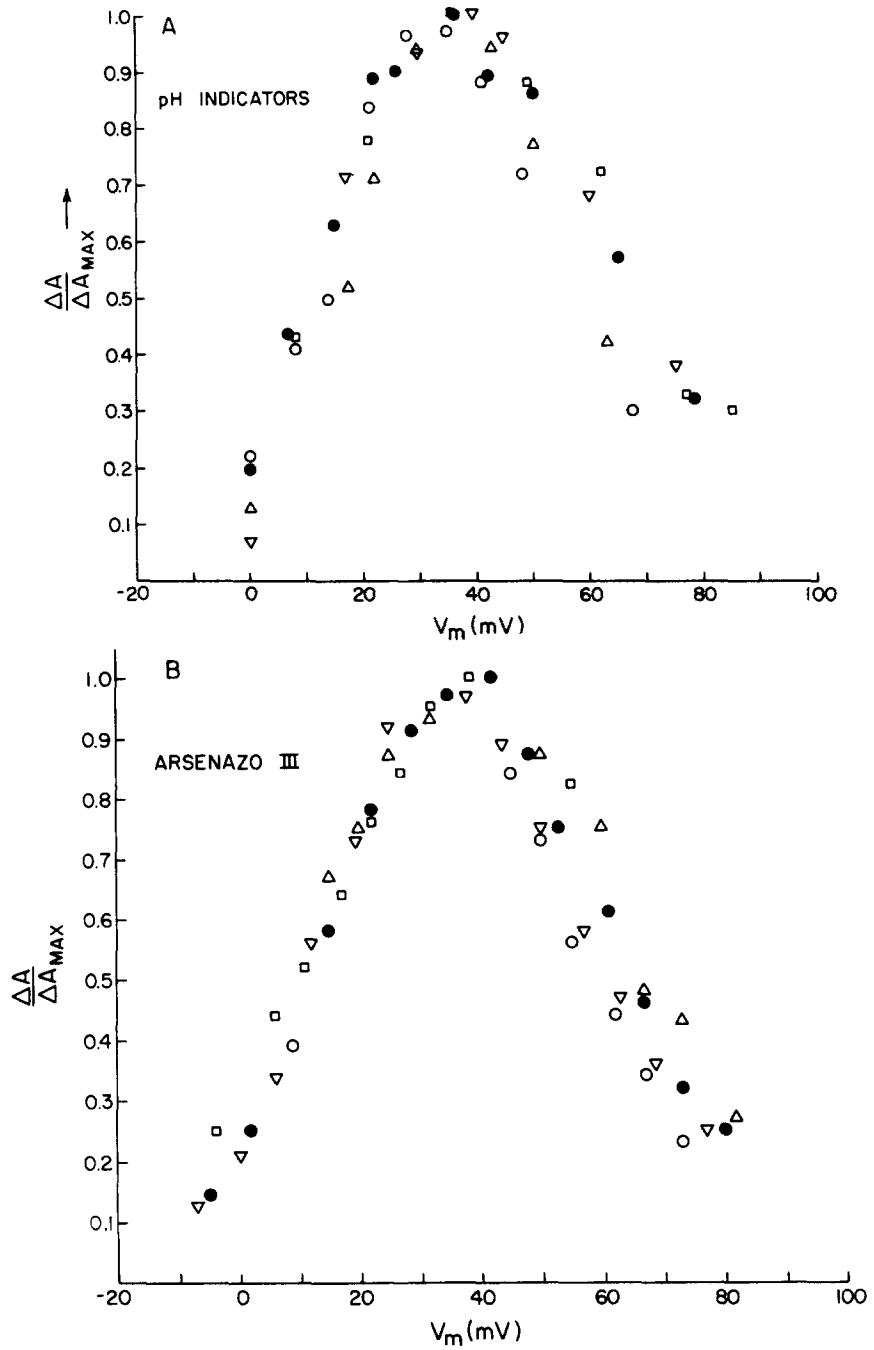

FIGURE 7. (A) Normalized pH indicator responses from five neurons vs. membrane voltage during voltage clamp pulses. The absorbance changes plotted were measured at the end of 1.2-s pulses and were corrected for base-line drift during the pulse. Indicator dye and normalization factors for ΔA are as follows: (○) BCP, 3.5×10^{-4}; (▽) PhR, 6×10^{-4}; (□) BCP, 3.8×10^{-4}; (△) BCP, 4×10^{-4}; (●) PhR, 5×10^{-4}. The maximum absorbance change, reached after the pulse termination, was approximately a factor of three greater than the value at the pulse end. (B) Normalized arsenazo III absorbance changes from five neurons vs. membrane voltage. Voltage clamp pulse duration and normalization factors for ΔA are as follows: (○) 375 ms, 3.8×10^{-3}; (□) 375 ms, 3×10^{-3}; (△) 250 ms, 2×10^{-3}; (●) 375 ms, 8.5×10^{-3}; (▽) 350 ms, 7.7×10^{-3}.

the two sets of data is obvious; both peak in the range +30–+40 mV and fall off rapidly to either side. Therefore, the size of the pH changes appears to be directly related to the amount of calcium influx. The arIII signals were measured using relatively brief pulses (<400 ms) to avoid interference from the delayed onset pH change which causes a decrease in the absorbance. Similar pH dye responses vs. V_m were obtained at external pH values of 6.8, 7.4, and 8.2.

The experiments illustrated demonstrate that the pH changes observed are closely linked to calcium movement but do not clearly show whether the immediate cause is the influx of divalent ions, calcium regulation, or some other factor secondarily related to either of these. The delayed onset and continuing change after the termination of Ca^{2+} influx would seem to favor one of the latter two choices. Experiments carried out with Ba substitution for Ca also suggest these possibilities. Barium ions substitute well for calcium as

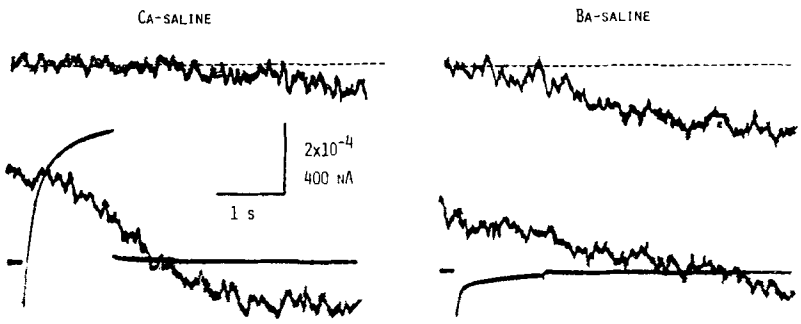

FIGURE 8. Effects of substituting 15 mM barium for 15 mM calcium in the external saline for identical voltage pulses. TEA was present in the external saline in both cases and the outward current was suppressed in barium saline. Base-line absorbance drift immediately before each pulse is shown in the top trace of each record.

carriers of transmembrane current in molluscan neurons as well as other excitable cells (c.f. Hagiwara, 1973; Keynes et al., 1973) but do not substitute well for calcium inside the cell. In particular, previous studies have indicated that Ba^{2+} does not appreciably activate the Ca-sensitive potassium conductance (Connor, 1979), nor is it removed from the cytoplasm at a rate anywhere near as fast as Ca^{2+} is (Ahmed and Connor, 1979 *a*). The data of Fig. 8 show that the pH indicator absorbance change is abolished by external substitution of Ba for Ca even though membrane current records show a net inward current which is carried by Ba. Previous work has shown that inward current is larger in Ba saline than in Ca saline for a given voltage pulse (Connor, 1979). The current waveforms are very different in the control-TEA vs. Ba-TEA runs because of the absence of Ca-activated potassium current in the Ba run. The base-line absorbance decrease was always greater in barium than in calcium saline and probably reflects an increased steady rate of acidification of the cytoplasm. The Ba record shown was made ~4 min after the switch of saline, well before a large acidification occurred.

Measurement of Cytoplasmic H^+ Buffering Capacity

Because pH_i of animal cells is strongly buffered, it is necessary to determine this buffering capacity before a quantitative relationship between internal calcium and pH can be established. We have estimated the pH buffering capacity in *Archidoris* neurons by three different methods: (I) measuring the pH change resulting from calibrated H^+ injection from a micropipette; (II) reduction of an activity-induced pH_i change by calibrated amounts of MOPS buffer; (III) measuring the cell pH_i change during voltage clamp of the

TABLE II

INTRACELLULAR PH BUFFERING CAPACITY

A. Method I

Cell (Date)	Path length	Dye concn	ΔA_{560}	ΔpH	H^+/HCO_3^- injected	Ion type injected	BC_{cell}
	cm	*mM*			*M*		*meq/unit pH per liter*
LPe_1 (7/19)	275×10^{-4}	0.95	0.0115	20.8×10^{-3}	5.4×10^{-4}	H^+(HCl)	26.0
RPe_2 (7/19)	300×10^{-4}	0.76	0.0042	8.6×10^{-3}	14.9×10^{-4}	H^+(HCl)	17.2
LPe_1 (7/20)	300×10^{-4}	0.60	0.0160	41.8×10^{-3}	3.2×10^{-4}	H^+(HCl)	7.7
RPe_2 (7/21)	250×10^{-4}	0.90	0.0045	9.4×10^{-3}	1.3×10^{-4}	H^+(HCl)	13.4
RPe_1 (7/21)	350×10^{-4}	0.94	0.029	41.5×10^{-3}	9.1×10^{-4}	H^+(HCl)	21.9
RPe_1* (7/27)	350×10^{-4}	0.45	0.014	41.8×10^{-3}	5.1×10^{-4}	H^+(HCl)	12.2
LPe_1‡ (7/28)	400×10^{-4}	0.50	0.022	51.7×10^{-3}	9.0×10^{-4}	HCO_3^-	17.4
RPl_1‡ (7/20)	350×10^{-4}	0.65	0.012	25.5×10^{-3}	1.13×10^{-4}	H^+(HCl)	4.4
LPl_1‡ (7/27)	400×10^{-4}	0.48	0.021	51.4×10^{-3}	3.32×10^{-4}	HCO_3^-	6.5
LPl_2 (7/24)	375×10^{-4}	0.65	0.012	22.3×10^{-3}	1.19×10^{-4}	$H^+(H_2SO_4)$	5.2
RPl_G (7/23)	400×10^{-4}	0.53	0.010	22.2×10^{-3}	1.25×10^{-4}	$H^+(H_2SO_4)$	5.7
RPl_G* (7/27)	450×10^{-4}	0.55	0.037	70.3×10^{-3}	5.30×10^{-4}	HCO_3^-	7.5
RPl_G* (7/28)	450×10^{-4}	0.57	0.039	71.5×10^{-3}	6.35×10^{-4}	HCO_3^-	8.9

B. Method II

Cell (Date)	Cell diameter	MOPS injected	BC MOPS	ΔA_{560} before MOPS	ΔA_{560} after MOPS	$\frac{\Delta pH_{init}}{\Delta pH_{MOPS}}$	BC_{cell}
	cm	*mM*	*meq/unit pH per liter*				*meq/unit pH per liter*
LPe_1 (9/29)	400×10^{-4}	23.2	7.48	0.001	0.0007	1.43	17.4
RPe_1 (7/28)	375×10^{-4}	22.5	7.26	0.002	0.0013	1.54	13.5
RPe_1 (8/1)	400×10^{-4}	32.0	10.32	0.0015	0.00089	1.69	15.1
LPl_1 (8/1)	425×10^{-4}	11.0	3.55	0.0014	0.00086	1.62	5.8
LPl_1 (9/29)	450×10^{-4}	16.0	5.16	0.0017	0.0007	2.43	3.6

* [PhR] measured with isotope. Iontophoretic injection of H^+/HCO_3^-. Transport no. for HCO_3^- = 0.3; for H^+ = 0.94.
‡ Absorbance used to measure [PhR]. Iontophoretic injection of H^+/HCO_3^-. No isotope used.

EGTA-injected neuron (c.f. Fig. 4) and estimating H^+ released from the *in situ* Ca-EGTA reaction and transmembrane calcium current. Results from methods I and II are summarized in Table II and show good agreement between methods for the values of buffering capacity, and an unexpected difference in capacity of cells from the pedal and pleural ganglia. Two experimental variations were performed under method I. Phenol red concentration was determined from absorbance measurements at $\lambda = 560$, and H^+ was injected under pressure and the amount determined by ^{35}S measurement. Alternatively, phenol red was injected under pressure along with ^{35}S for concentration

measurement, and H^+ or HCO_3^- was injected iontophoretically with transport numbers of 0.94 and 0.3 used to estimate the amount (see Thomas, 1976). Injection electrodes contained either 2 M HCl or $KHCO_3$.

Fig. 9 shows the ΔpH_i resulting from action potential trains in two neurons under normal conditions and after partial elimination by MOPS buffer, pressure injected along with ^{35}S (method II). The pH change resulting from the spike train in Fig. 9 A was 3×10^{-3} U in the control run, and that for the train of Fig. 9 B, 4×10^{-3} U. Buffering capacity of the cell was computed on the assumption of linear summation of intrinsic buffer capacity (BC_{cell}) and added exogenous buffer capacity (BC_{MOPS}). This assumption leads to the

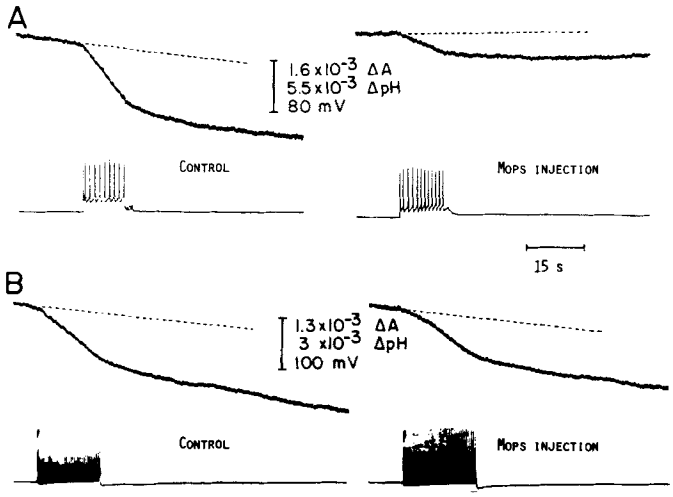

FIGURE 9. Reduction of endogeneous pH response by injected MOPS buffer. (A) Cell LP_{l1} showing the pH response to action potential train before and after the injection of MOPS (15 mM). V_m was clamped at −45 mV before and after spike train. (B) Similar experiment in cell RPe_1 where 22 mM MOPS produced a smaller relative suppression.

expression:

$$BC_{cell} = \frac{BC_{MOPS}}{\frac{\Delta pH_{init}}{\Delta pH_{MOPS}} - 1},$$

where ΔpH_{init} is the pH change before MOPS injection and ΔpH_{MOPS} is the smaller change following injection. Buffer capacity of MOPS solutions at concentrations between 10 and 30 mM was measured in the internal saline solution (Table I). It increased linearly with concentration going from 3.1–9.3 meq/unit pH per liter over this concentration range.

The third method (EGTA) is the most indirect and involves making an estimate of $Ca^{2+}:H^+$ stoichiometry *in situ*. Furthermore, the EGTA may have side effects that distort the results, and the measurements are necessarily carried out with $[Ca]_{in}$ lower than normal. Nevertheless, we considered the

measurements worthwhile because the technique gives a more rapid increase of H^+ than the other two methods and a more spatially uniform increase than method I. H^+ released per Ca^{2+} bound by EGTA was 2:1 in in vitro measurements (see Materials and Methods). Assuming this same 2:1 stoichiometry *in situ*, and that the EGTA bound all transmembrane calcium influx, the buffering capacity of seven neurons tested ranged between 20 and 60 meq/unit pH per liter. This method did not show significant differences between pedal and plural neurons. It is not clear at present why the estimates from method III are higher than those from methods I and II.

The intrinsic buffering capacities of PhR and BCP were measured in vitro and were 0.45 and 1.0 meq/unit pH per liter, respectively, at 1 mM dye concentration. At concentrations of 0.5–1.0 mM, the range generally employed *in situ*, phenol red should make a contribution to total H^+ buffering capacity of the cell of $< 10\%$.

The arIII Response and the Measurement of $[Ca^{2+}]$ *during pH Changes*

It was reported previously (Ahmed and Connor, 1979 *a*) that injection of EGTA into the cytoplasm abolished the arIII signal or reversed its direction. The initial observations were made before the extent and time-course of the pH_i change were fully appreciated and the spectral dependence of the signal was not investigated. Fig. 10 extends these observations by showing arIII absorbance records at three wavelengths, before and after EGTA injection, and demonstrates in a direct manner the interrelation of Ca and pH effects on arIII. Identical voltage pulses were used for all six runs. Under control conditions (Fig. 10 A) the arIII signal increased at both 610 and 660 nm with the signal at 660 being the larger of the two. Near the isosbestic point, 580 nm, the absorbance change was relatively small. After EGTA injection (Fig. 10 B), the 660-nm signal was reduced to ~7% of the control signal and its direction reversed to an absorbance decrease. The 610-nm signal was also reversed after EGTA injection but now was the larger of the two signals. Extrapolating from the pH and Ca indicator data, the intracellular conditions are as follows: in the control runs $[Ca^{2+}]_{in}$ begins to rise almost immediately after the pulse onset and pH_i starts to drop 200–400 ms later; after EGTA injection $[Ca^{2+}]_{in}$ is clamped to a very low level even during Ca^{2+} influx and pH_i begins a larger total drop immediately after the pulse onset. The factors producing the absorbance change in the latter case are then a pH change in the presence of an appreciable Mg concentration. The wavelength dependence under the conditions of EGTA injection, then, should be a combination of a Mg·arIII − arIII difference spectrum, since Mg is the predominant ion to be displaced by the increased $[H^+]$, and pH difference spectrum for arIII. Both these difference spectra have a peak around 600–610 nm and fall off at longer wavelengths. Because of the relative sizes of the absorbance changes, the Mg difference spectrum should be the more important of the two. With EGTA present the arIII then acts primarily as a pH indicator because $[Ca^{2+}]$ changes are negligible, whereas normally it monitors both Ca and pH. As noted in a preceding study (Ahmed and Connor, 1979 *a*), the control 610-nm signal

decayed much faster than the one at 660, and this is primarily because of the larger influence of pH change at 610 nm.

The membrane currents in the EGTA runs show a systematic increase in the tendency to decay toward zero; the order of runs was 610, 660, and 580

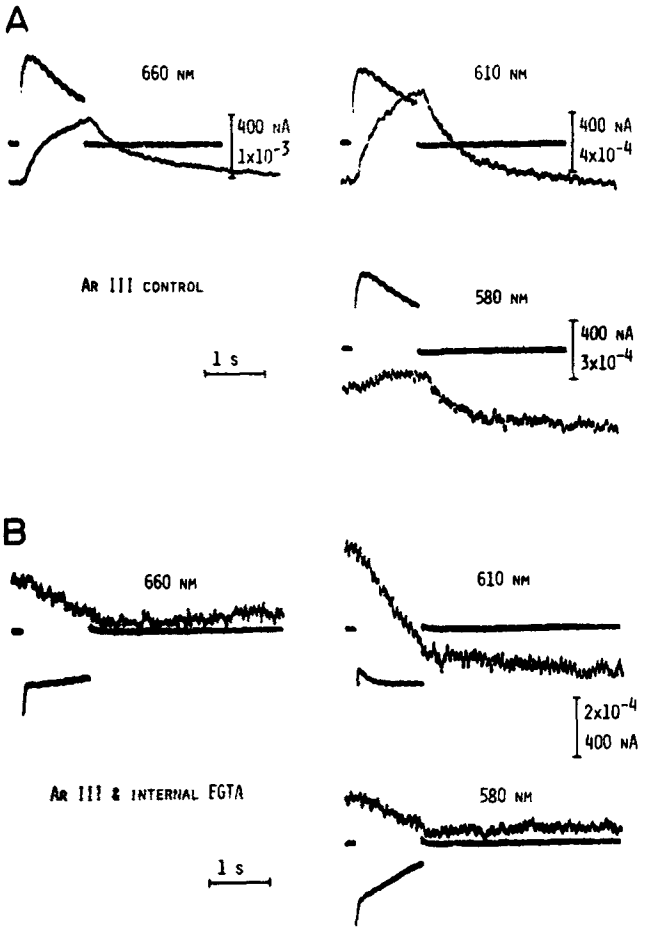

FIGURE 10. Response of internal arsenazo III in the absence (A) and presence (B) of internal EGTA. Identical voltage pulses (+25 mV) elicited the responses throughout. (A) Simultaneous current records (upper beam) and absorbance (lower beam) are shown at three wavelengths. The slight lag in the absorbance response is due to the filter time constant in the optical system (50 ms) and a misalignment of the oscilloscope beams. (B) Current and absorbance records after injection of EGTA (ca. 2 mM) into the neuron of A. The absorbance beam has been shifted upward for these records since the direction of change reversed. External saline contained TEA. Cell: $RP/_1$.

nm. This was commonly observed for small doses of EGTA (<1 mM) and probably represents partial saturation of the chelating agent in the later runs.

At pH values around neutrality, hydrogen ions readily replace either calcium or magnesium in the arIII complex. Where one or the other of these

is the only divalent ligand present, magnesium in the example above, the pH difference spectrum is approximately that of the ligand −arIII difference spectrum (see Fig. 3, Ahmed and Connor, 1979 *a* for pH effect with only Ca present). The effect of lowering pH with either Mg or Ca, or both, present is to decrease dye absorbance at wavelengths between 580 and 700 nm. *In situ*, however, we have determined that a pH_i decrease causes the 660-nm absorbance of arIII to increase. Internal pH has been decreased by CO_2 exposure and by injection of H^+ with the same qualitative effects. Fig. 11 shows simultaneous absorbance changes at 660 and 610 nm resulting from H^+ injection. Onset and termination of the injection are indicated by arrows. During the first 30–40 s of the injection period, the arIII absorbance decreased at both wavelengths, with the decrease at 610 nm being much more pro-

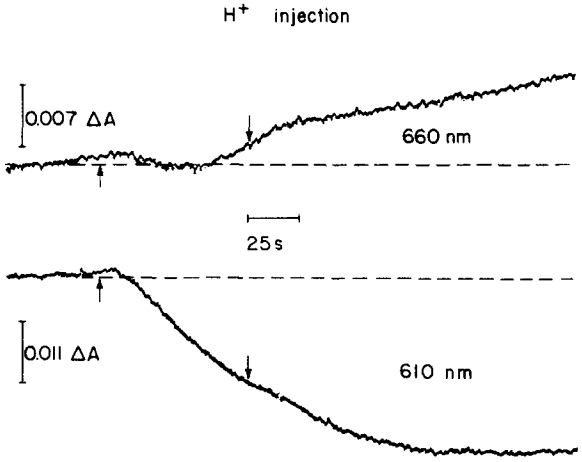

FIGURE 11. Simultaneous tracking of arsenazo III absorbance changes at 660 and 610 nm during and after the iontophoretic injection of H^+. Arrows mark onset and termination of injection. This record was taken before recovery from a prior injection had occurred and both base lines show an upward tilt.

nounced than the one at 660 nm, as expected for a simple pH change. Subsequently, the 660-nm signal reversed direction and began to increase while the 610-nm signal continued to decrease. Both absorbance signals continued to change well after the injection was terminated. Thus, during this latter period, the *in situ* dye absorbance at 660 nm changed in the opposite direction to in vitro experiments where pH was lowered, or to *in situ* experiments where pH was lowered but $[Ca^{2+}]$ was buffered (Fig. 10). Therefore, we conclude that the injection of H^+ caused an increase in internal $[Ca^{2+}]$. The 610-nm absorbance behaved the same as in vitro experiments, presumably because pH and Mg effects on dye absorbance outweigh the $[Ca^{2+}]$ influence at this wavelength.

DISCUSSION

The measurements reported here demonstrate the time-course of pH changes that develop during neural activity and give cause for relating them to changes

in internal calcium concentration. These pH changes are very small and we accordingly refrain from ascribing possible physiological effects to them at this point. Because the neurons have a considerable H^+ buffering capacity, however, the small pH changes result from a fairly large release of protons and one should not ignore the fact that a large portion of the released protons have reacted with cytosolic systems which may be involved in some yet unknown physiological function. Apart from this the measured pH changes may be of some value in sorting out the different mechanisms involved in calcium and pH regulation.

The results also demonstrate an apparent reciprocal relationship between internal calcium and pH inasmuch as a decrease in internal pH produced an increase in the internal calcium level. This latter observation has also been made by Lea and Ashley (1978) in barnacle muscle and may have considerable bearing on the interpretation of behavior in cells forced into conditions of relative acidity or alkalinity by various physiological disorders or experimental procedures. With our present experimental measurements the size of the pH change responsible for the $[Ca^{2+}]$ increase can only be estimated from mean values of buffer capacity, 16 meq/unit pH per liter for pedal cells and 6 meq/unit pH per liter for pleural cells (from Table II), and the amount of H^+ injected during an experiment, estimated from iontophoretic current. Using these data the acidification necessary to produce an increase in A_{660} of arsenazo III ranged from 0.2 to 0.5 U pH in 10 neurons examined. Finally, the results illustrate some of the problems, and potentials, the use of metal indicators such as arsenazo III present.

When spike trains were used as a stimulus as in Figs. 5 and 9, it is possible that some of the pH change was due to increased metabolic activity set off by increases in $[Na]_i$ and decreases in $[K]_i$ (c.f. DeWeer, 1975). Under voltage clamp, however, the contribution of $[Na]_i$ changes should be negligible because an appreciable sodium current flows only during the first few milliseconds of the clamp. With regard to $[K]_i$, the addition of TEA did not decrease the pH signal under voltage clamp although this agent greatly reduced potassium current. Action potentials in TEA saline were much broader than in control saline and were accompanied by pH changes much larger than control.[1]

The measured values for H^+ buffering capacity (see Table II) are in fair agreement with the 10.7 meq/unit pH per liter value reported by Thomas (1976) for *Helix* neurons, although our data show considerable scatter and two populations of neurons. A comparison can also be made with the study of Meech and Thomas (1977) in which Ca^{2+} was injected into *Helix* neurons through a microelectrode and the resulting pH change measured. The stoichiometry of the relation, injected $Ca^{2+}:H^+$ increase, was approximately 1:1 for calcium loads that approached 1 mM. In our experiments the transmembrane calcium current during a large voltage clamp pulse ($+10 < V_{clamp} < +30$) was typically 60–100 $\mu A/cm^2$ figured on an equivalent sphere basis. Therefore pulses of 1.3 s duration should impose calcium loads of approxi-

[1] Ahmed, Z., and J. A. Connor. Unpublished observations.

mately 50–80 μM in a 500-μm cell assuming steady influx during the pulse. Using this range of calcium load, a pH buffering capacity (BC) of 10 meq/unit pH per liter, and the 1:1 stoichiometry for $Ca^{2+}:H^+$ of Meech and Thomas, one calculates an expected pH_i change of 5×10^{-3} to 8×10^{-3} unit from the equation $BC = \Delta[H^+]/\Delta pH$. This range of values is somewhat higher than the pH changes reported here but within the same order of magnitude. Conversely a somewhat lower ratio for the $Ca^{2+}:H^+$ ratio would be calculated from our data.

Realistically, the indicator absorbance changes measured in this study cannot be translated into pH_i changes with an uncertainty of less than a factor of 2, given geometric irregularities of the cells and the problems of measuring dye concentration. Moreover, it should be stressed that in making the translation at all, it has been implicitly assumed that pH_i is uniform over the cell interior since the effective optical pathlength used is equal to the cell diameter. If for some reason the pH_i changes are partitioned radially by diffusion lags or internal membranes, actual compartmental pH changes will be larger than those reported here.

The limitations of the indicator dye method were tolerated to make measurements of small, rapid pH_i changes during electrical activity. Such changes cannot be tracked by glass microelectrodes because of the inherently long time constants involved. For example, the pH electrodes employed in this study were very large but still had an electrical time constant of several seconds. Smaller electrodes will have a longer electrical time constant, and those with recessed sensing tips (Thomas, 1974, 1976) introduce a considerable diffusion delay into the response time for a pH change. During period where V_m undergoes change and during action potentials or a voltage clamp pulse, the KCl microelectrode, but not the pH electrode, will be able to track the voltage changes. The difference signal will then have a large, non-pH component which disappears only after V_m has been maintained at a steady level for periods which are several time constants of the pH electrode.

We thank Doctors T. Ebrey and R. Gennis for helpful discussions and for making available the equipment used in some of the in vitro measurements. We are grateful to Dr. L. Pinto for helpful discussion on cleaning the pH-indicators. We also thank Ms. L. Kragie for technical assistance.

Supported by grant GB 39946 from the National Science Foundation and grants NS-15181 and RR-07030 from the National Institutes of Health, U.S. Public Health Service.

Received for publication 16 February 1979.

REFERENCES

AHMED, Z., and J. A. CONNOR 1979 *a*. Measurement of calcium influx under voltage clamp in molluscan neurons using the metallochromic dye arsenazo III. *J. Physiol. (Lond.)*. **286**:61–82.

AHMED, Z., and J. A. CONNOR. 1979 *b*. Buffering of internal H^+ in neurons. *Biophys. J.* **25**:265a. (Abstr.)

BORON, W. F., and P. DEWEER. 1976. Intracellular pH transients in squid giant axons caused by CO_2, NH_3, and metabolic inhibitors. *J. Gen. Physiol.* **67**:91–112.

BRINLEY, F. J., and A. SCARPA. 1975. Ionized magnesium concentration in axoplasm of dialyzed squid axons. *FEBS. Fed. Eur. Biochem. Soc. Lett.* **50:**83–85.

BROWN, H. M., R. W. MEECH, and R. C. THOMAS. 1976. pH changes induced by light in large *Balanus* photoreceptors. *Biophys. J.* **16:**33a. (Abstr.)

BROWN, H. M., and R. W. THOMAS. 1978. Intracellular injection of H^+ and HCO_3^- in *Balanus* photoreceptor. *Biophys. J.* **21:**117a. (Abstr.)

BROWN, J. E., P. K. BROWN, and L. H. PINTO. 1977. Detection of light induced change of intracellular ionized calcium concentration in *Limulus* ventral photoreceptors using arsenazo III. *J. Physiol. (Lond.).* **267:**299–320.

CALDWELL, P. C. 1958. Studies on the internal pH of large muscle and nerve fibres. *J. Physiol. (Lond.).* **142:**22–62.

CHANCE, B. 1972. Principles of differential spectrophotometry with special reference to dual wavelength. *Methods Enzymol.* **24:**321–335.

COLE, K. S., and J. W. MOORE. 1960. Liquid junction and membrane potentials of the squid giant axon. *J. Gen. Physiol.* **43:**971–980.

COLES, J. A. and J. E. BROWN. 1976. Effects of increased intracellular pH buffering capacity on the light response of *Limulus* ventral photoreceptor. *Biochem. Biophys. Acta.* **436:**140–153.

CONNOR, J. A. 1979. Calcium current in molluscan neurones: measurement under conditions which maximize its visibility. *J. Physiol. (Lond.).* **286:**41–60.

CONNOR, J. A., and Z. AHMED. 1978. Colorimetric determination of calcium and pH changes under voltage clamp in molluscan neurons. *Biophys. J.* **21:**186a. (Abstr.)

CONNOR, J. A., and Z. AHMED. 1979. Intracellular calcium regulation by molluscan neurons. *Biophys. J.* **25:**265a. (Abstr.)

DEWEER, P. 1975. Aspects of the recovery processes in nerve. *MTP (Med. Tech. Publ. Co.) Int. Rev. Sci. Ser. One Physiol.* **3:**231–278.

HAGIWARA, S. 1973. Ca spike. *Adv. Biophys.* **4:**71–102.

KEYNES, R. D., E. ROJAS, R. E. TAYLOR, and J. VERGARA. 1973. Calcium and potassium systems of a giant barnacle muscle fibre under membrane potential control. *J. Physiol. (Lond.).* **229:** 409–455.

LEA, T. J., and C. C. ASHLEY. 1978. Increase in free Ca^{2+} in muscle after exposure to CO_2. *Nature (Lond.).* **275:**236–238.

MCDONALD, V. W., and F. F. JÖBSIS. 1976. Spectrophotometric studies on the pH of frog skeletal muscle: pH change during and after contractile activity. *J. Gen. Physiol.* **68:**179–195.

MEECH, R. W. 1974. The sensitivity of *Helix aspersa* neurones to injected calcium ions. *J. Physiol. (Lond.).* **237:**259–277.

MEECH, R. W., and R. C. THOMAS. 1977. The effect of calcium injection on the intracellular sodium and pH of snail neurones. *J. Physiol. (Lond.).* **265:**867–879.

PAILLARD, M. 1972. Direct intracellular pH measurement in rat and crab muscle. *J. Physiol. (Lond.).* **223:**297–319.

SPYROPOULOS, C. S. 1960. Cytoplasmic pH of nerve fibres. *J. Neurochem.* **5:**185–194.

THOMAS, R. C. 1974. Intracellular pH of snail neurones measured with a new pH-sensitive glass micro-electrode. *J. Physiol. (Lond.).* **238:**159–180.

THOMAS, R. C. 1976. The effect of carbon dioxide on the intracellular pH and buffering power of snail neurones. *J. Physiol. (Lond.).* **255:**715–735.

WADDELL, W. J., and R. G. BATES. 1969. Intracellular pH. *Physiol. Rev.* **49:**285–329.